

Relaxation and Metastability in the Random WalkSAT search procedure

Guilhem Semerjian^{1,*} and Remi Monasson^{1,2,†}¹CNRS-Laboratoire de Physique Theorique de l'ENS, 24 rue Lhomond, 75005 Paris, France.²CNRS-Laboratoire de Physique Theorique, 3 rue de l'Universite, 67000 Strasbourg, France.

(Dated: October 27, 2019)

An analysis of the average properties of a local search resolution procedure for the satisfaction of random Boolean constraints is presented. Depending on the ratio of constraints per variable, resolution takes a time T_{res} growing linearly ($T_{\text{res}} \propto N$; $\alpha_d < 1$) or exponentially ($T_{\text{res}} \propto \exp(N^\alpha)$; $\alpha_d > 1$) with the size N of the instance. The relaxation time τ_{res} in the linear phase is calculated through a systematic expansion scheme based on a quantum formulation of the evolution operator. For $\alpha_d > 1$, the system is trapped in some metastable state, and resolution occurs from escape from this state through crossing of a large barrier. An annealed calculation of the height Φ of this barrier is proposed. The polynomial/exponential cross-over α_d is not related to the onset of clustering among solutions.

I. INTRODUCTION

The study of combinatorial problems [1] with statistical physics techniques started almost twenty years ago [2]. Most of the efforts have been devoted to the calculation of the optimal solution of various problems (traveling salesman, matching, graph or number partitioning, satisfiability of Boolean constraints, vertex cover of graphs...) as a function of the definition parameters of their inputs distributions. Central to these studies is the characterization of the properties of the extrema of correlated random variables, a question of considerable importance in probability theory [3]. From a computer science point of view, however, the main point is the characterization of resolution times. Concepts and tools issued from the analysis of algorithms have allowed so far to understand the behaviour and the efficiency of many algorithms of practical use [4, 5], sorting for instance, but progress has been much slower in the analysis of search procedures for combinatorial problems. These are sophisticated algorithms hardly amenable to rigorous analysis with available techniques [6]. Statistical physics ideas and approximation techniques may then be of great relevance to help develop quantitative understanding and intuition about the operation of these algorithms. To some extent, the study of algorithms may be seen as part of out-of-equilibrium statistical physics.

There exists a wide variety of algorithms for combinatorial problems [1]. Roughly speaking, two main classes may be identified. The first one includes complete algorithms, guaranteed to provide the optimal solution. They essentially consist in an exhaustive albeit clever (making use of branch and bound procedures) search through the conformation space, and may require very large computational times, i.e. scaling exponentially with the size of the inputs to be treated. Recently, notions borrowed from statistical physics as real-space renormalization and out-of-equilibrium growth processes allowed to reach some understanding of the operation of complete algorithms for the satisfiability [7, 8] and the vertex cover [9, 10] problems over random classes of inputs. Incomplete algorithms constitute another large class of resolution procedures: they may be able to find the optimal solution very quickly, but may also run forever without ever finding it. An example is provided by local procedures e.g. Monte Carlo dynamics which attempt at finding a solution from an arbitrary initial conformation through a sequence of stochastic local moves in the conformation space. When specialized to decision problems (for which the desired output is the answer YES or NO to a question related to the inputs, as: is there a way to color a given graph with 7 colors only?), local search algorithms can sometimes be made one-sided error probabilistic algorithms [11]. When they stop, the answer is YES with certainty. If they run for a time t without halting, the probability (over the non deterministic choices of local moves in the conformation space) that the correct answer is NO is bounded from below by a function $f(t; N)$ going to 1 when $t \rightarrow \infty$. Obviously this function depends on the size N of the input: the larger the input, the larger the time $t_c(N)$ it takes to reach, say, a 99% confidence that the answer is NO i.e. $f(t_c(N); N) = 0.99$. Determining the scaling (polynomial or exponential) of $t_c(N)$ with N is of capital importance to assess the efficiency of the algorithm.

In this paper, we study this question for a local search procedure, the Random WalkSAT algorithm [12], and a decision problem defined over an easy-to-parametrize class of inputs, the random satisfiability problem [13]. Both procedure and problem are defined in Section II. We also recall the main results proven by mathematicians on these

*Electronic address: guilhem@lpt.ens.fr

†Electronic address: monasson@lpt.ens.fr

issues, and present an overview of the phenomenology of Random WalkSAT. A major theoretical interest for studying the Random WalkSAT algorithm is that it is, apparently, of purely dynamical nature. Detailed balanced is indeed verified in a trivial way: the equilibrium measure is non zero over solutions only, and the transition rates from a solution to any other configuration are null. The equilibrium measure is therefore of no use to understand long time dynamics, a situation reminiscent of some models studied in out-of-equilibrium physics e.g. the contact process for finite size systems [14]. We are thus left with a study of the dynamical evolution of a spin system with disorder in the interactions (the instances of the combinatorial problem to be solved are random), a still largely open problem in statistical physics [15]. We show in Section III how the master equation for this evolution can be written as a Hamiltonian (in imaginary time) for 1/2 quantum spin systems, and use this representation to get exact results and develop systematic expansions for the quantities of interest, valid in some region of the parameter space. In Section IV, we present an approximate analysis of the Random WalkSAT procedure in the whole parameter space. We show that, depending on the value of the ratio of the number of constraints per (Boolean) degree of freedom, resolution is either achieved in linear time or requires the escape from some metastable region in the configuration space, a slow process taking place over exponentially large times. Interestingly, the dynamics generated by Random WalkSAT is very similar to the physical dynamics of (spin) glassy systems [15]. Some perspectives are presented in Section V. Note that a complementary study of the Random WalkSAT procedure was very recently carried out by Barthel, Hartmann and Weigt [16].

II. DEFINITIONS, KNOWN RESULTS AND PHENOMENOLOGY

A. The random K-Satisfiability problem

The 3-Satisfiability (3-SAT) decision problem is defined as follows. Consider a set of N boolean variables x_i , $i = 1, \dots, N$. A literal is either a variable x_i or its negation \bar{x}_i . A clause is the logical OR between 3 distinct literals. It is thus true as soon as one of the literals is true. A formula is the logical AND between M clauses, it is true if and only if all the clauses are true. A formula is said to be satisfiable if there is an assignment of the variables such that the formula is true, unsatisfiable otherwise.

3-SAT is a NP-complete problem [1]; it is believed that there is no algorithm capable of solving every instance of 3-SAT in a time bounded from above by a polynomial of the size of the instance. How well do existing and a priori exponential algorithms perform in practice? To answer these questions, computer scientists have devised a simple way of generating random instances of the 3-SAT problem, with a rich pattern of hardness of resolution [13]. Formulas are drawn in the following way. Repeat M times independently the same process: pick up a 3-uplet of distinct indices in $[1; N]$, uniformly on all possible 3-uplets. For each of the 3 corresponding variables, choose the variable itself or its negation with equal probability ($1/2$), and construct a clause with the chosen literals. Repetition of this process M times gives a set of M independently chosen clauses, whose conjunction is the generated instance. The random generation of formula makes the set of possible formulas a probability space, with a well defined measure.

Numerical experiments indicate that a phase transition takes place when $N/M \rightarrow 1$ at fixed ratio $\alpha = M/N$ of clauses per variables (in the thermodynamic limit). If α is smaller than some critical value $\alpha_c \approx 4.3$, a randomly drawn instance admits at least one solution with high probability. Beyond this threshold, instances are almost never satisfiable. The existence of this transition has not been proven rigorously yet [17], but bounds on the threshold exist: the probability of satisfaction tends to 1 (respectively to 0) if $\alpha < 3.42$ [18] (resp. $\alpha > 4.506$ [19]). All the above definitions can be extended to the K -SAT problem, where each clause is the disjunction of K , rather than 3, literals. 2-SAT is an easy (polynomial) problem, while K -SAT is NP-Complete for any $K \geq 3$. Location of the threshold is rigorously known for 2-SAT ($\alpha_c = 1$) [20] but not for $K \geq 3$. We shall denote in the following averages on the random K -SAT ensemble by $\langle \dots \rangle_K$.

Statistical mechanics studies have pointed out the existence of another phase transition taking place in the satisfiable phase ($\alpha < \alpha_c$) with a location, first estimated to $\alpha_s \approx 3.95$ [21] and then to $\alpha_s \approx 3.92$ [22]. This phase transition is related to the microscopic structure of the set of solutions. Define the Hamming distance between two solutions as the number of variables taking opposite values in these solutions. When $\alpha < \alpha_s$, there exist an exponentially large (in N) number of solutions, each pair of which are separated by a path in the solution space, that is, a sequence of solutions with a $O(1)$ Hamming distance between successive solutions along the path. The solution space is made of a single cluster of solutions. For $\alpha < \alpha_s$, the solution space breaks into an exponentially large (in N) number of clusters, separated by large voids of solutions. Two solutions in one cluster are linked through a path while there is no path in the solution space linking two solutions in two different clusters. This clustering phenomenon, whose discovery was inspired from previous works in the context of information storage in neural networks [23], was subsequently found in various combinatorial problems [24, 25], and rigorously demonstrated for the so-called random XORSAT problem [26]. It is a zero temperature signature of the ergodicity breaking taking place in spin glasses [15, 27].

Its precise relationship with dynamical properties, and in particular with the computational cost for finding a solution is not fully elucidated yet [21, 22, 28].

B . The Random WalkSAT algorithm

The operation of Random WalkSAT (also called Random Walk) on an instance of the K -SAT problem is as follows [12].

1. Choose randomly a con guration of the Boolean variables.
2. If all clauses are satis ed, output "Satis able".
3. If not, choose randomly one of the unsatis ed clauses, and one of the K variables of this clause. Flip the variable. Notice that the selected clause is now satis ed, but the ip operation may have violated other clauses which were previously satis ed.
4. Go to step 2, until a limit on the number of ips fixed beforehand has been reached. Then Output "Don't know".

What is the output of the algorithm? Either "Satis able" and a solution is exhibited, or "Don't know" and no certainty on the status of the formula is reached. Papadimitriou showed that Random WalkSAT solves with high probability any satis able 2-SAT instance in a number of steps (ips) of the order of N^2 [12]. Recently Schoning was able to prove the following very interesting result for 3-SAT [29]. Call 'trial' a run of Random WalkSAT consisting of the random choice of an initial con guration followed by $3N$ steps of the procedure. If none of T successive trials of Random WalkSAT on a given instance has been successful (has provided a solution), then the probability that this instance is satis able is lower than $\exp(-T(3=4)^N)$. In other words, after $T(4=3)^N$ trials of Random WalkSAT, most of the con guration space has been 'probed': if there were a solution, it would have been found. Though Random WalkSAT is not a complete algorithm, the uncertainty on its output can be made as small as possible and it can be used to prove unsatis ability (in a probabilistic sense).

Schoning's bound is true for any instance. Restriction to special input distributions allows to improve his result. Alekhnovich and Ben-Sasson showed that instances drawn from the random 3-Satis ability ensemble described above are solved in polynomial time with high probability when α is smaller than 1.63 [30]. It is remarkable that, despite the quenched character of the disorder in this problem (the same clauses are seen various times in the course of the search), rigorous results on the dynamics of this spin model can be achieved.

C . Phenomenology of the operation of Random WalkSAT

In this section, we briefly sketch the behaviour of Random WalkSAT, as seen from numerical experiments [31] and the analysis presented later in this article. We find that there is a dynamical threshold α_d separating two regimes:

for $\alpha < \alpha_d \approx 2.7$ for 3-SAT, the algorithm finds a solution very quickly, namely with a number of ips growing linearly with the number of variables N . Figure 1A shows the plot of the fraction f_0 of unsatis ed clauses as a function of time t (number of ips divided by M) for one instance with ratio $\alpha = 2$ and $N = 500$ variables. The curves show a fast decrease from the initial value ($f_0(t=0) = 1/8$ in the large N limit independently of α) down to zero on a time scale $t_{res} = O(1)$. Fluctuations are smaller and smaller as N grows. t_{res} is an increasing function of α . This relaxation regime corresponds to the one studied by Alekhnovich and Ben-Sasson, and $\alpha_d > 1.63$ as expected [30]. Figure 2A symbolizes the behaviour of the system in the relaxation regime.

for instances in the $\alpha_d < \alpha < \alpha_c$ range, the initial relaxation phase taking place on $t = O(1)$ time scale is not sufficient to reach a solution (Figure 1B). The fraction f_0 of unsat clauses then fluctuates around some plateau value for a very long time. On the plateau, the system is trapped in a metastable state. The life time of this metastable state (trapping time) is so huge that it is possible to define a (quasi) equilibrium probability distribution $p_N(f_0)$ for the fraction f_0 of unsat clauses. (Inset of Figure 1B). The distribution of fractions is well peaked around some average value (height of the plateau), with left and right tails decreasing exponentially fast with N , $p_N(f_0) \sim \exp(-N(f_0 - \langle f_0 \rangle)^2)$ with $\langle f_0 \rangle = 0$ (Figure 2B). Eventually a large negative fluctuation will bring the system to a solution ($f_0 = 0$). Assuming that these fluctuations are independent random events occurring with probability $p_N(0)$ on an interval of time of order 1, the resolution time is a stochastic variable with exponential distribution. Its average is, to leading exponential order, the inverse of the probability of resolution on the $O(1)$ time scale: $[t_{res}] \sim \exp(N)$ with $\alpha = 0$. Escape from the metastable state therefore occurs through barrier

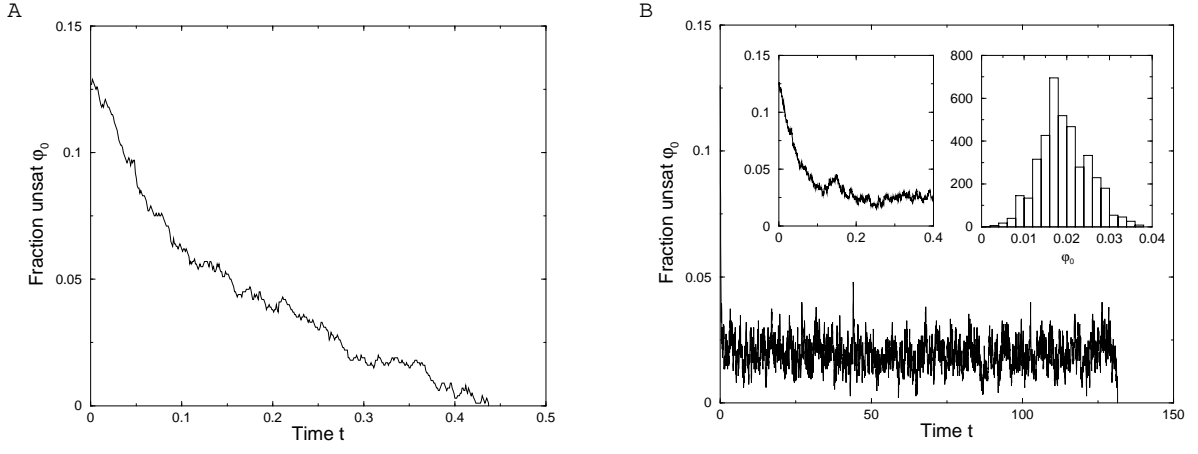


FIG. 1: Fraction ϕ_0 of unsatisfied clauses as a function of time t (number of steps over M) for two randomly drawn instances of 3-SAT with ratios $\alpha = 2$ (A) and $\alpha = 3$ (B) with $N = 500$ variables. Note the difference of time scales between the two figures. Insets of figure B: left: blow up of the initial relaxation of ϕ_0 , taking place on the $O(1)$ time scale as in (A); right: histogram $p_{500}(\phi_0)$ of the fluctuations of ϕ_0 on the plateau for $t > 130$.

crossing and takes place on exponentially large $\{N\}$ time scales, as confirmed by numerical simulations for different sizes. Schoning's result[29] can be interpreted as a lower bound to the probability $\phi_0 > \ln(3/4)$, true for any instance.

The plateau energy, that is, the fraction of unsatisfied clauses reached by Random WalkSAT on the linear time scale is plotted on Figure 3. Notice that the "dynamic" critical value α_d above which the plateau energy is positive (Random WalkSAT stops finding a solution in linear time) is strictly smaller than the "static" ratio α_c , where formulas go from satisfiable with high probability to unsatisfiable with high probability. In the intermediate range $\alpha_d < \alpha < \alpha_c$, instances are almost surely satisfiable but Random WalkSAT needs an exponentially large time to prove so. Interestingly, α_d and α_c coincides for 2-SAT in agreement with Papadimitriou's result[12]. Furthermore, the dynamical transition is apparently not related to the onset of clustering taking place at α_s .

III. EXACT RESULTS: SPECIAL CASES AND EXPANSIONS

A. Evolution equations and quantum formalism

Boolean variables will be hereafter represented by Ising spins, $S_i = 1$ (resp. -1) when the Boolean variable x_i is true (resp. false). A microscopic configuration S is specified by the states of all variables: $S = (S_1; S_2; \dots; S_N)$. We then define a 2^N dimensional linear space with canonical basis $\{|\mathbf{S}\rangle\}$, orthonormal for the scalar product $\langle \mathbf{S}^0 | \mathbf{S} \rangle = \prod_i \delta_{S_i^0, S_i}$. Let us denote $\text{Prob}[\mathbf{S}; T]$ the probability that the system configuration is S at time T i.e. after T steps of the algorithm, and define [32]

$$|\mathbf{S}(T)\rangle = \sum_{\mathbf{S}} \text{Prob}[\mathbf{S}; T] |\mathbf{S}\rangle \quad (1)$$

as the (time-dependent) vectorial state of the system. Knowledge of this vector gives access to the probability $\text{Prob}[\mathbf{S}; T] = \langle \mathbf{S}^0 | \mathbf{S}(T) \rangle$ of being in a certain configuration S .

Random WalkSAT defines a Markov process on the set of configurations; during one step of the algorithm the state vector of the system changes according to

$$|\mathbf{S}(T+1)\rangle = \hat{W}_d |\mathbf{S}(T)\rangle \quad (2)$$

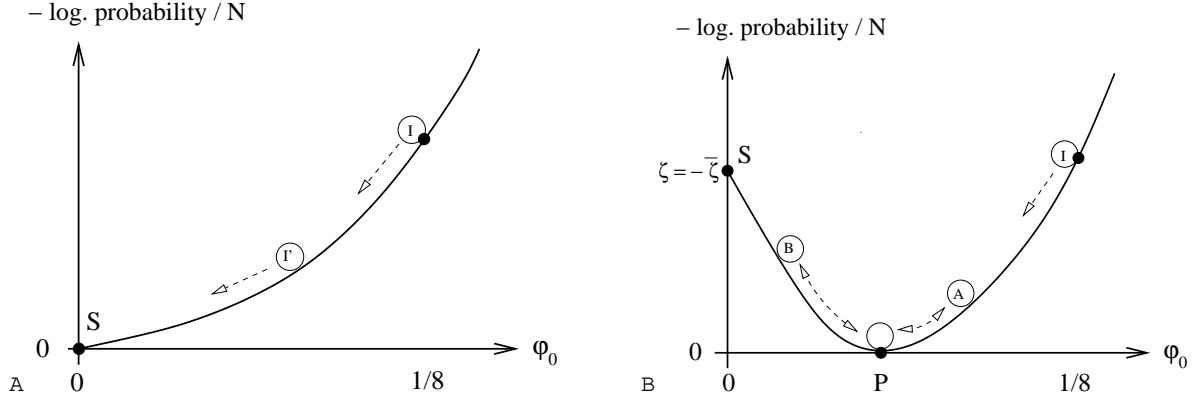


FIG. 2: Schematic picture of the operation of Random WalkSAT for ratios smaller (A) or larger (B) than the dynamical threshold α_d . Vertical axis is minus the logarithm of the probability (divided by N) that the system has a fraction ϕ_0 of unsat clauses after a large number of Random WalkSAT steps. Its representative curve can be seen as an energy potential in which the configuration (represented by an empty ball) rolls down towards the more probable value of the order parameter ϕ_0 , or up, through stochastic fluctuations. The starting configuration violates $\phi_0 = 1/8$ of the clauses (point I). At small ratios (A), the configuration rolls down to reach point S through a sequence of intermediary points (I'). Resolution is essentially a fast relaxation towards S ($O(1)$ time scale). At large ratios (B), the ball first relaxes to the bottom of the well (point P with abscissa corresponding to the plateau height). Then slow negative (ball A) or positive (ball B) fluctuations of the fraction ϕ_0 take place on exponentially (in N) long time scales. The time $t_{res} \sim \exp(N)$ it takes to the system to reach a solution (point S) is, on the average, equal to the inverse probability $\exp(N)$ that a fluctuation drives the system to S.

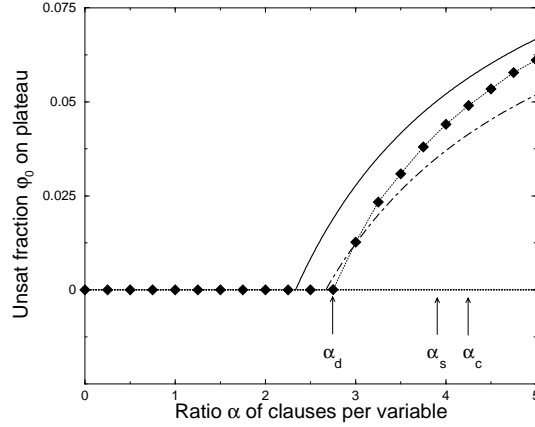


FIG. 3: Fraction ϕ_0 of unsatisfied clauses on the metastable plateau as a function of the ratio of clauses per variable. Diamonds are the output of numerical experiment, and have been obtained through average of data from simulations at a given size N (nb. of variables) over 1,000 samples of 3-SAT, and extrapolation to infinite sizes (dotted line serves as a guide to the eye). The ratio at which ϕ_0 begins being positive, $\alpha_d \approx 2.7$, is smaller than the thresholds $\alpha_s \approx 3.9$ and $\alpha_c \approx 4.3$ above which solutions gather into distinct clusters and instances have almost surely no solution respectively. Dot-dashed and full lines represent the predictions of the Markovian approximation of Section IV C and IV E respectively.

where the evolution operator in discrete time \hat{W}_d reads

$$\hat{W}_d = \prod_{i=1}^M \hat{F}_i \hat{U} \hat{E}^{-1}; \quad \hat{F}_i = \frac{1}{K} \sum_{j=1}^N C_{ij}^2 \sigma_i^x; \quad \hat{U} = \sum_{j=1}^N C_{1j} \sigma_j^z; \quad \hat{E} = \prod_{i=1}^M \hat{U}_i; \quad (3)$$

In the above expression, we have made use of several new notations that we now explain. The $M \times N$ matrix C_{ij} encodes the instance: C_{ij} equals 1 if the j -th clause contains the literal x_i , -1 if it contains the literal \bar{x}_i , and 0 otherwise. Since every clause contains K literals, $\sum_{i=1}^N C_{ij}^2 = K$. The Pauli operators are defined through $\sigma_i^z \beta_i = S_i \beta_i$, and $\sigma_i^x \beta_i = \beta_i^{\dagger} \beta_i$, where S_i is the configuration obtained from S by flipping the i -th spin. It is a simple

check that the argument of function g_K in \hat{U} is a diagonal operator in the canonical basis \mathcal{B} , with eigenvalues $x = \prod_{i=1}^N C_i S_i$ in $\{-K; -K+2; \dots; K-2; K\}$, equal to K if and only if clause ℓ is unsatisfied. The function

$$g_K(x) = x; K = \frac{1}{2^K K!} \sum_{p=0}^{K-1} (K-2p-x) \quad (4)$$

is a polynomial of degree K in x equal to 1 if $x = K$ and to zero for all the other possible eigenvalues. Operator \hat{E} is diagonal in the canonical basis too, with eigenvalues equal to the numbers of unsatisfied clauses (also called energy) in each configuration. Therefore $\hat{U} \cdot \hat{E}^{-1}$ in (3) acts as a filter retaining clause ℓ only if it is unsatisfied, and with a weight equal to the inverse number of unsatisfied clauses: only unsat clauses can be chosen at each time step, each of them with the same probability. \hat{F}_ℓ flips the spins of clause ℓ , each with probability $1/K$. Notice that \hat{W}_d conserve probabilities: $\langle \hat{W}_d \rangle = \langle \hat{W} \rangle$ where $\langle \hat{W} \rangle = \sum_s \langle \hat{W} \rangle_s$ is the superposition of all possible states.

In the thermodynamic limit, the evolution can be rewritten in continuous time, defining $t = T/M$,

$$\frac{d}{dt} \mathcal{P}(t) = \hat{W} \mathcal{P}(t) \quad ; \quad \hat{W} = M (\hat{W}_d - \hat{I}) \quad (5)$$

Formally, the solution of this equation is $\mathcal{P}(t) = e^{t\hat{W}} \mathcal{P}(0)$, where $\mathcal{P}(0) = (1/2^N) \sum_i \mathcal{P}_i$ since the initial configuration is random. An important quantity to compute is the average fraction of unsatisfied clauses at time t , i.e. after $T = Mt$ steps of the algorithm, averaged both on the history of the algorithm and on the distribution of formulas:

$$r_0(t) = \frac{1}{M} \sum_i \langle \hat{E} e^{t\hat{W}} \mathcal{P}(0) \rangle_i \quad (6)$$

For the sake of analytical simplicity, we shall study a slightly different evolution operator in the next two subsections, and use the parameter u to denote the time parameter of this modified evolution,

$$\hat{W}^0 = \hat{W} - \frac{1}{M} \hat{E} = \sum_{\ell=1}^M \hat{F}_\ell - \hat{I} - \hat{U} \quad ; \quad \frac{d}{du} \mathcal{P}(u) = \hat{W}^0 \mathcal{P}(u) \quad (7)$$

Let us explain the meaning of this modification. The operator \hat{W}^0 would have been obtained starting from the following variant of the Random WalkSAT stochastic process. At each step, choose a clause among the M ones. If it is satisfied, do nothing. If it is unsatisfied, flip one of its variables.

In the thermodynamic limit, the fraction of unsatisfied clauses r_0 is expected to become a self-averaging quantity, i.e. to be peaked with high probability around its (time-dependent) mean value. Turning \hat{W} into \hat{W}^0 thus amounts to a local redefinition of time, independent of the instance of the problem. In definition (7), the operator \hat{E}/M can be replaced with its mean value r_0 , leading to $\frac{d}{du} \mathcal{P} = r_0 \frac{d}{dt}$. The knowledge of the \hat{W}^0 evolution of any observable in terms of u can then be rewritten in terms of t through

$$t(u) = \int_0^u du' r_0(u') \quad : \quad (8)$$

Examples of this time reparametrization will be shown below.

B. The $K = 1$ case

Let us first study the simple case $K = 1$. A clause is then a single literal, i.e. either a variable or its negation. If both a variable and its negation appear in the formula, it is obviously unsatisfiable. This is the case, with high probability in the thermodynamic limit, as soon as $\alpha > 0$. Static properties of 1-SAT model are known exactly [33], and its dynamics under the Random WalkSAT evolution can be solved too.

An instance is described by a set of integers $\{m_i; n_i\}$, where m_i is the number of clauses in which the variable i appears, and $(m_i - n_i)/2$ is the number of times it has been chosen without negation. The evolution operator in terms of u (time is the sum of site-operators

$$\hat{W}_i^0 = \frac{1}{2} (m_i x_i - m_i + n_i z_i - n_i x_i z_i) \quad (9)$$

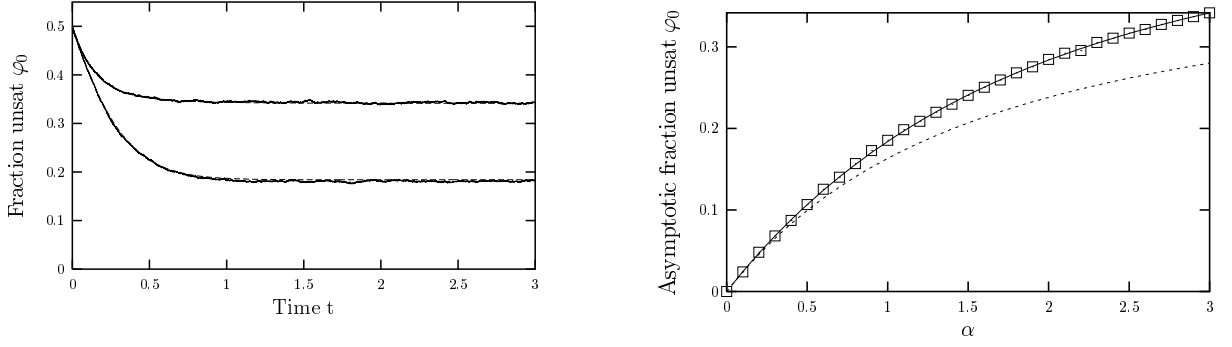


FIG. 4: Comparison between numerical and analytical results for $K = 1$. Left panel: fraction of unsat clauses $f_0(t)$ as a function of time t for $\alpha = 3$ (top) and $\alpha = 1$ (bottom). Dashed line: analytical curve, solid line (almost superimposed): numerical results (single run with $N = 10^4$). Right panel: asymptotic fraction of unsat clauses as a function of α , solid line: theoretical prediction (13), symbols: numerical results (averaged over 10 runs, over $t \in [8;10]$, for $N = 10^4$), dashed line: groundstate energy f_{GS} .

As the operators \hat{W}_i^0 on different sites commute, the evolution operator can be diagonalized in each of the i subsets independently, and the vector state is a tensor product,

$$\mathcal{P}(u)_i = \prod_{i=1}^N \frac{1}{2} \sum_{s=1}^2 \left(\frac{1}{2} (j_i + j_{-i}) \right) \begin{cases} 1 & \text{if } m_i = 0 \\ e^{m_i u} & \text{if } m_i \neq 0 \end{cases} \mathcal{P}_i \quad (10)$$

where $j_{\pm i}$ are the eigenvectors of \hat{W}_i^z with eigenvalues ± 1 . The fraction of unsatisfied clauses for a given instance and averaged over the choices of the algorithm reads,

$$\frac{1}{M} \text{tr} \hat{\mathcal{P}} \mathcal{P}(u)_i = \frac{1}{2} \left(\frac{1}{2M} \sum_{i=m_i \neq 0} \frac{n_i^2}{m_i} - 1 \right) e^{m_i u} \quad (11)$$

In the thermodynamic limit, the m_i 's become independent random variables with identical Poisson distributions of parameter α ; $(m_i - n_i)/2$ obeys a Binomial law of parameter $1/2$ among m_i . Performing the quenched average over the formula, the fraction of unsatisfied clauses reads

$$f_0(u) = \frac{1}{2} \left(\frac{1 - \exp(-(e^u - 1))}{2} \right) \quad (12)$$

These exact results are compared with numerical simulations in Figure 4. On the right panel has been drawn the asymptotic fraction of unsatisfied clauses obtained at large times, compared with the analytical prediction made above. The left panel shows the time evolution of the fraction of unsatisfied clauses as a function of time t , for two different values of α . The analytical curve has been obtained through the rescaling explained at the end of the previous subsection: from the exact value of $f_0(u)$ given above, the original time $t(u)$ has been obtained by numerical integration (eqn. (8)), and the plot $f_0(t)$ is a parametric plot $f(t) = t(u); f_0 = f_0(u)$, parametrized by u .

Note that the asymptotic value of the energy reached is larger than the groundstate one [33],

$$\lim_{t \rightarrow \infty} f_0(t) = \frac{1}{2} + \frac{e}{2} \left(\frac{1}{2} - \frac{1}{2} \right) = \frac{1}{2} (1 - e^{-I_0(\alpha)} - e^{-I_1(\alpha)}) = f_{GS} \quad (13)$$

where I_n is the n -th modified Bessel function. This is easily understood: if a formula contains x_1 once and x_1 twice, the optimal value is $x_1 = \text{false}$. But the algorithm does not stop in this configuration, as the clause x_1 is then violated. Random WalkSAT will keep on flipping the variable and make the average energy higher than the optimal one.

C. The satisfiable phase of the $K = 2$ case

We now turn to the 2-SAT case, where every clause involves two variables. It has been rigorously proven that there is a sharp threshold phenomenon taking place at $\alpha_c = 1$ in this problem [20]: for lower values of α the formulas are

almost always satisfiable, beyond this threshold they are almost always unsatisfiable. The dynamical critical threshold of Random WalkSAT has the same value, $\phi_d = 1$ [12]. Thus there is no metastability in 2-SAT: if a solution of the formula exists it is almost surely found in polynomial time. Two questions of interest are: how fast will the number of unsatisfiable clauses decrease during the evolution of the process and how long will it take the algorithm to find a solution for $\phi < 1$? What will be the typical energy after a long run of the algorithm when $\phi > 1$? In this and the next subsections we shall address the first of these two questions, and leave the second one to the next section.

As in the $K = 1$ case, one can use the quantum formalism and write down the evolution operator \hat{W}^0 . There appear both single site terms and couplings between pairs of sites,

$$\hat{W}^0 = \prod_i \hat{W}_i^0 + \prod_{i \neq j} \hat{W}_{ij}^0 \quad (14)$$

$$\hat{W}_i^0 = \frac{1}{8} (m_i x_i x_i + m_i + 2n_i z_i z_i + n_i x_i z_i) \quad (15)$$

$$\hat{W}_{ij}^0 = \frac{1}{8} a_{ij} \frac{x_i^2 + x_j^2}{2} + 1 z_i z_j + b_{ij} x_i z_j \quad (16)$$

with

$$n_i = \prod_{\ell} C_{i\ell} ; \quad m_i = \prod_{\ell} C_{i\ell}^2 ; \quad a_{ij} = \prod_{\ell} C_{i\ell} C_{j\ell} ; \quad b_{ij} = \prod_{\ell} C_{i\ell}^2 C_{j\ell} \quad (17)$$

Two-sites operators \hat{W}_{ij}^0 do not commute when they share a variable, and \hat{W}^0 cannot be factorized as in the $K = 1$ case. Yet, a cluster expansion in powers of ϕ can be implemented. A detailed presentation of this cluster expansion in a closely related context has been given elsewhere [34]; the reader is referred to this previous work for more details. The method is presented below for a generic value of K . We call cluster and denote F_r a maximal set of variables connected by clauses. Any formula F can be decomposed as a conjunction of these clusters (note that despite the similarities in denominations, these clusters have nothing to do with the clustering phenomenon in configuration space). Consider now a quantity Q , depending of the realization of the disorder, namely of formula F , and additive with respect to the clusters decomposition, $Q(F) = \prod_{F_r} Q(F_r)$. Calculation of the average $\langle Q \rangle$ over the random ensemble formulas of Q can be done as follows. First, consider the different possible topologies of the clusters, compute $\langle Q \rangle_s$, the quantity averaged over the choices of signs for a given topology i.e. whether variables appear negated or not in a clause. Secondly, add up these contributions with combinatorial factors giving the frequency of appearance of the different topologies,

$$\frac{1}{M} \langle Q \rangle = \sum_s \frac{1}{L_s} P_s \langle Q \rangle_s \quad (18)$$

The sum runs over the different topologies, L_s is the number of sites in such a cluster, and P_s is the probability of a given site belonging to an s -type cluster. In the thermodynamic limit, the finite-size clusters which contribute to this sum are tree-like: $P_s = (K!)^{m_s} e^{-L_s K} K_s$, where $m_s = (L_s - 1)/(K - 1)$ is the number of clauses of the cluster, and K_s a symmetry factor. The smallest tree-like clusters are shown in Figure 5. Clauses are represented by dashed lines (for $K = 2$) or stars (for $K = 3$). In principle, such an expansion is meaningful only below the percolation threshold of the underlying random hypergraph, $\phi_p = 1/(K - 1)$. Beyond ϕ_p , a giant component appears, whereas the series (18) takes into account clusters of size $O(\ln N)$ only. However, rearranging the series as an expansion in powers of ϕ (expanding out the exponential in P_s) allows to extend its domain of validity beyond ϕ_p , at least for quantities that are not singular at the percolation threshold.

This method can be employed here: the evolution operator \hat{W}^0 is a sum of operators for each cluster $\hat{W}^0(F_r)$. Operators attached to two distinct clusters commute with each other as they do not have common variables. The energy operator \hat{E} can also be written as a sum over the clusters, thus the energy averaged over the history of the algorithm has the property of additivity over clusters if the time evolution is studied in terms of u . After averaging over the formulas, the fraction of unsatisfied clauses reads,

$$\langle f_0(u) \rangle = \sum_s \frac{1}{L_s} P_s \langle f_0(u) \rangle_s \quad (19)$$

The evolution and energy operators for a cluster with n variables are $2^n \times 2^n$ matrices, \hat{W}_s^0 and \hat{E}_s respectively. With the help of a symbolic computation software one can easily study the small finite-size clusters by computing

$$\langle f_0(u) \rangle_s = \frac{1}{h_0} \text{Tr} \left[\hat{E}_s e^{\hat{W}_s^0 u} f_0(0) \right] \quad (20)$$

Type	L_s	K_s	$\langle \mathbb{E} i(u) \rangle_s$	$\langle t_{res} \rangle_s$
a	2	1	$\frac{1}{4}e^{-u}$	1=4
b	3	3=2	$\frac{1}{16}e^{-2u} + \frac{5}{16}e^{-u} + \frac{1}{8}e^{-u=2}$	19=32
c	4	2	$\frac{1}{128}e^{-3u} + 10e^{-2u} + 4e^{-3u=2} + 53e^{-u} + 20e^{-u=2} + 2(2 - \frac{p}{2})e^{-\frac{2+p}{2}u} + 2(2 + \frac{p}{2})e^{-\frac{2-p}{2}u}$	125=128
d	4	2=3	$\frac{3}{256}e^{-3u} + 10e^{-2u} + 25e^{-u} + 32e^{-u=2}$	259=256

TABLE I: Contributions to the cluster expansions for $K = 2$. See left panel of Figure 5.

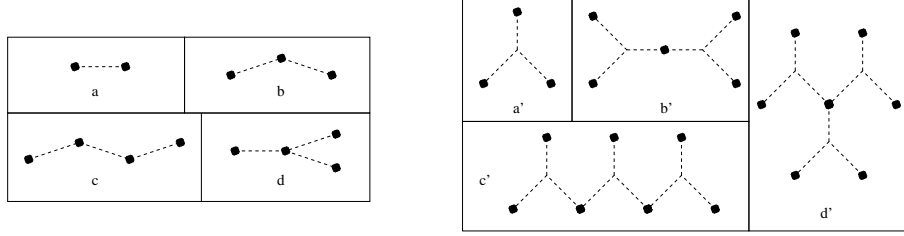


FIG. 5: Tree-like clusters contributing to the expansions. Left panel: $K = 2$. Right panel: $K = 3$.

where \mathbf{h} and \mathbf{j} are now 2^n row and column vectors, and the average is over the choices of negating or not the variables in the clauses.

We have performed this task for clusters with up to four sites, their contributions are summarized in Table I. Up to order 2^2 , the expansion leads to

$$\begin{aligned}
 \rho_0(u) = & \frac{e^{-u}}{4} + \frac{1}{4}e^{-u=2} - \frac{3}{8}e^{-u} + \frac{1}{8}e^{-2u} \\
 & + 2 \left(\frac{3}{8}e^{-u=2} + \frac{19}{64}e^{-u} + \frac{1}{8}e^{-3u=2} - \frac{9}{32}e^{-2u} + \frac{3}{64}e^{-3u} \right) \\
 & + 2 \left(\frac{p-3}{32}e^{-\frac{3+p}{2}u} - \frac{p-3+1}{32}e^{-\frac{3-p}{2}u} + \frac{2}{16}e^{-\frac{2+p}{2}u} + \frac{2+p}{16}e^{-\frac{2-p}{2}u} \right) + O(2^3) \quad (21)
 \end{aligned}$$

The typical value $\rho_0(t)$ of the fraction of unsatisfied clauses after $T = tM$ steps of the algorithm is obtained from (21) through the rescaling of time defined in eqn. (8). Our theory is compared in Figure 6 to numerical simulations. The agreement is excellent at the beginning of the time evolution, and worsens at the end. A factor of explanation is that during the last steps of the algorithm, the fraction of unsatisfied clauses is low and thus for finite-size samples, the self-averaging hypothesis is violated.

Our approach is applicable to any value of K (note however that the size of the matrices to be diagonalized grows faster with the number of clauses in the clusters studied, that is, with the order in 2^n in the expansion) but is restricted to the $<_d$ regime. The finite-size tree clusters considered at any (finite) order in the expansion are indeed solved in linear time by Random WalkSAT. In Section IV, another kind of approximation will allow to study the $>_d$ regime.

D. Cluster analysis of resolution times

As the number of steps needed to solve a formula is an additive quantity over clusters, it can be calculated along the lines exposed above for the expansion of ρ_0 . Let us give two examples about how to compute the average time needed to solve a cluster of fixed topology.

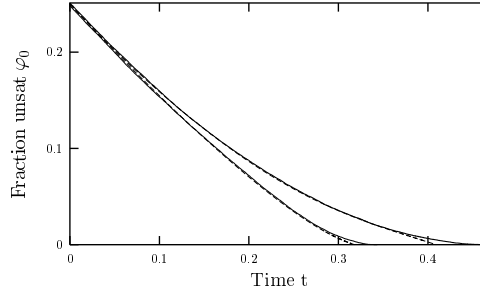


FIG. 6: Fraction of unsat clauses as a function of time for $K = 2$, $\alpha = 0.6$ (top) and $\alpha = 0.3$ (bottom). Dashed lines: cluster expansion prediction, solid lines (almost superimposed): numerical results (averaged over 10 runs for $N = 10,000$).

The simplest example is a cluster made of a single 2-SAT clause, $(x_1 \vee x_2)$. With probability $3/4$, the initial random condition is already a solution. If not, it will take one time step to solve the cluster, as any of the two possible spins will lead to a solution. Thus the average resolution time is $1/4$. Similar analysis can be done on bigger clusters, even if the counting becomes increasingly tiresome. As a byproduct, some flaws of the Random WalkSAT heuristic appear.

The second example is the cluster $(x_1 \vee x_2) \wedge (x_2 \vee x_3)$. The eight configurations of the variables are represented in Figure 7 with up or down spins corresponding to true or false boolean variables. The four solutions are drawn in the shaded box. Two configurations are turned into solutions in one step (single outgoing arrow). Flip of a spin from each of the remaining two configurations (with two departing arrows), leads to a solution, or to the other configuration. Thus the average resolution time starting from one of these configurations is two time steps. Finally, the average resolution time for the cluster is $3/4$. To obtain the average over the signs of this resolution time, one still has to make the same study for the case where the two clauses are not contradictory on the central spin, hence the value $19/32$ on line b of Table I.

Obviously, Random WalkSAT can make "bad" choices on this very simple example, and "oscillate" a few time steps between the two configurations before finding a solution. One can imagine many local search heuristics which would do better than Random WalkSAT on the example shown before. For instance, one could modify the algorithm so that once an unsatisfied clause has been chosen randomly, it picks preferably a variable with a low number of neighbors, or one with the lowest number of contradicting clauses on it. The average resolution time of any of these heuristics, as long as the information used to choose the variable to be flipped remains local, can be studied by such a cluster expansion. These simple enumerations could then provide an useful test ground for new heuristics.

For general K , the enumeration of the possible histories of clusters with three or less clauses leads to the quantities given in Table II,

$$t_{\text{res}}(\alpha; K) = \frac{1}{2^K} + \frac{K(K+1)}{K} \frac{1}{1} \frac{1}{2^{2K+1}} + \frac{4K^6 + K^5 + 6K^3}{3(K-1)(2K-1)(K^2-2)} \frac{10K^2 + 2K}{2} \frac{1}{2^{3K+1}} + O(\alpha^3) \quad (22)$$

This prediction is in good agreement with numerical simulations, see Figure 8 for results in the $K = 3$ case.

The validity of expression (22) can be easily checked for $K = 2$ from the findings of Section IIIC. Indeed, in terms of the time $t = T/M$, the fraction of unsat clauses $\phi_0(t)$ vanishes after a finite time t_{res} given by

$$t_{\text{res}} = \lim_{u \rightarrow 1} \int_0^u t(u) du = \int_0^1 t(u) du \quad (23)$$

Integration of (21) coincides with prediction (22) for $t_{\text{res}}(\alpha; 2)$.

IV. APPROXIMATE ANALYSIS OF RANDOM WALKSAT

In this section, an analysis of Random WalkSAT, based on a Markovian approximation for the evolution equations (2) is proposed. It allows a quantitative description of the main features of Random WalkSAT, namely the asymptotic

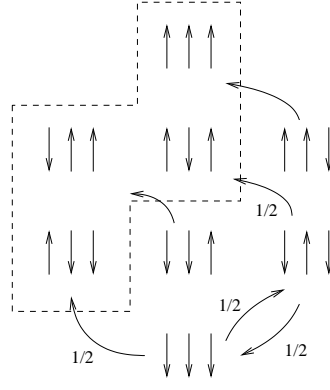


FIG. 7: An example of the behaviour of Random WalkSAT on a finite cluster $(x_1 \wedge x_2) \wedge (x_2 \wedge x_3)$. Blocks of spins represent configurations of the boolean variables, those in the shaded box are solutions. Arrows stand for possible transitions of the algorithm, see the text for details.

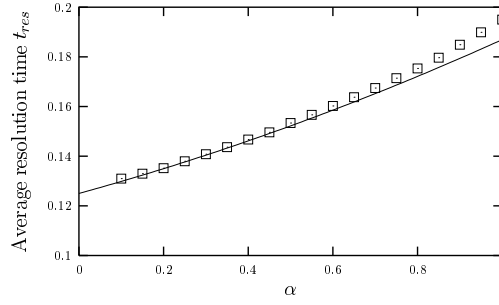


FIG. 8: Average resolution time $t_{res}(\alpha; 3)$ for 3-SAT. Symbols: numerical simulations, averaged over 1,000 runs for $N = 10,000$. Solid line: prediction from the cluster expansion (22).

energy and the (exponentially small) probability of resolution in linear time for generic values of K and α_d . The approximation scheme is also applied to the analysis of Random WalkSAT on the XOR SAT problem [35].

A. Projected evolution

Consider an instance of the K -SAT problem. Random WalkSAT defines a Markov process on the space of configurations of the Boolean variables, see eqn. (2), of cardinality 2^N . Call $S(T)$ the configuration of the Boolean variables at a given instant T (number of steps) of the evolution of the algorithm. An observable R is a function of the configuration e.g. the number of clauses violated by S . The principle of the approach developed now is to track the evolution of $R(T) = R(S(T))$, that is, of one number (or a low-dimensional vector) instead of the whole configuration of spins. To do so, we make use of the projection operator formalism exposed below.

Let us partition the configuration space into equivalence classes of microscopic configurations S associated to the

Type	L_s	$K_s(K!)$	$m_s = L_s$	t_{res}^s
a^0	K	1		$\frac{1}{2^K}$
b^0	$2K$	1	$\frac{K^2}{2}$	$\frac{1}{2^{2K}} \left(2^{K+1} + \frac{K+1}{K(K-1)} \right)$
c^0	$3K$	2	$\frac{K^3(K-1)}{2}$	$\frac{1}{2^{3K}} \left(3 \cdot 2^K + 2^{K+1} \frac{K+1}{K(K-1)} + \frac{4K^4 + 9K^3 + 9K^2 + 6K - 4}{3K^2(K-1)(2K-1)} \right)$
d^0	$3K$	2	$\frac{K^3}{6}$	$\frac{1}{2^{3K}} \left(3 \cdot 2^K + 2^K \frac{3(K+1)}{K(K-1)} + \frac{2K+1}{K^2(K-1)} \right)$

TABLE II: Contributions to the cluster expansion for the resolution time, general K . See right panel of Figure 5.

same value of the macroscopic observable $R(S)$. We call $(R) = \{S \in \mathcal{R} \mid R(S) = R\}$ these classes, and $j(R)$ their cardinalities (number of configurations in these classes). Let us define the projection operator \hat{P} through its entries,

$$\langle S_1 | \hat{P} | S_2 \rangle = \frac{1}{j(R(S_1))} \langle R(S_1) | R(S_2) \rangle ; \quad (24)$$

where $\langle \cdot | \cdot \rangle$ denotes the (vectorial) Kronecker function. One can easily check that it is indeed a projector, $\hat{P}^2 = \hat{P}$, which connects only configurations within the same class.

Now consider the state vector $|\mathcal{P}(T)\rangle$ and its projection $|\hat{\mathcal{P}}(T)\rangle = \hat{P} |\mathcal{P}(T)\rangle$. Its components have the same value in each class, which is the average of $|\mathcal{P}(T)\rangle$ over the microscopic configurations in the class. Call $|\mathcal{Q}(T)\rangle = (1 - \hat{P}) |\mathcal{P}(T)\rangle = |\mathcal{P}(T)\rangle - |\hat{\mathcal{P}}(T)\rangle$. From the master equation (2), we obtain

$$\begin{aligned} |\mathcal{P}(T+1)\rangle &= \hat{P} \hat{W}_d |\mathcal{P}(T)\rangle + \hat{P} \hat{W}_d |\mathcal{Q}(T)\rangle \\ |\mathcal{Q}(T+1)\rangle &= (1 - \hat{P}) \hat{W}_d |\mathcal{P}(T)\rangle + (1 - \hat{P}) \hat{W}_d |\mathcal{Q}(T)\rangle \end{aligned} \quad (25)$$

The second equation can be formally "integrated" by iteration,

$$|\mathcal{Q}(T)\rangle = \sum_{T^0=1}^{T^T} ((1 - \hat{P}) \hat{W}_d)^{T^0} |\mathcal{P}(T - T^0)\rangle \quad (26)$$

where the initial state vector $|\mathcal{P}(0)\rangle$ has been assumed to be uniform on each class, so that $|\mathcal{Q}(0)\rangle = 0$. Finally,

$$|\mathcal{P}(T+1)\rangle = \sum_{T^0=0}^{T^T} \hat{P} \hat{W}_d ((1 - \hat{P}) \hat{W}_d)^{T^0} |\mathcal{P}(T - T^0)\rangle \quad (27)$$

Equation (27) expresses that, once coarse-grained by the action of the projection operation, the dynamics is not Markovian any longer. The principle of our approximation is precisely to omit all memory effects, by neglecting non Markovian terms i.e. $T^0 \geq 1$ contributions in (27), and averaging over disorder at each time step,

$$|\mathcal{P}(T+1)\rangle \approx \hat{P} \hat{W}_d |\mathcal{P}(T)\rangle \quad (28)$$

Obviously, the quality of the approximation depends on the observable R . We shall see two examples in what follows.

B. Transition matrix for the number of unsatisfied clauses

A natural choice we study in this and the next two subsections for the observable R is M_0 , which measures the numbers M_0 of clauses unsatisfied by each configuration of the variables. Defining the bra

$$\langle M_0 | j \rangle = \sum_{S \in \mathcal{M}_0} \langle S | j \rangle ; \quad (29)$$

and the probability $\text{Prob}[M_0; T] = \langle M_0 | \mathcal{P}(T) \rangle$ that the configuration of the variables is in class M_0 at time T , we obtain within the Markovian approximation (28),

$$\text{Prob}[M_0; T+1] = \sum_{M_0} A_{M_0^0 M_0} \text{Prob}[M_0^0; T] ; \quad (30)$$

with $A_{M_0^0 M_0} = N_{M_0^0 M_0} / D_{M_0}$ and

$$\begin{aligned} N_{M_0^0 M_0} &= \sum_{j=1}^{X^N} \sum_{S \in \mathcal{M}_0} \langle M_0^0 | S \rangle \langle M_0 | S^j \rangle p_j(S) \\ D_{M_0} &= \sum_S \langle M_0 | S \rangle \end{aligned} \quad (31)$$

where $p_j(S)$ is the probability of flipping spin k when the system is in configuration S i.e. the number of unsatisfied clauses in which spin j appears divided by the number of unsat clauses. S^j denotes the configuration obtained from

S by flipping spin j . The meaning of our Markovian approximation is clear: the transition rate from one value of the observable M_0 to another is the average of the microscopic transition rates from one microscopic conformation belonging to the first subset (M_0) to another belonging to the second one, with a flat average on the starting subset. At time T , the only available information in the projected process is that the system is somewhere in the subset, and none of the corresponding microscopic conformations can be privileged.

To perform the average over the disorder, i.e. on the random distribution of formulas and compute $[A_{M_0^0 M_0}] = [N_{M_0^0 M_0} / D_{M_0}]$, we shall do the further approximation that the numerator and the denominator can be averaged separately. This 'annealed' hypothesis can be justified in some cases, see Section IV G. After some combinatorics, we find

$$[A_{M_0^0 M_0}] = \sum_{Z_u, Z_s} \frac{X}{K M_0} \frac{Z_u N}{K M_0} \frac{M_0}{Z_u} \frac{M}{Z_s} \frac{M_0}{Z_s} \frac{1}{N} \frac{K^{M_0 Z_u}}{N} \frac{K^{Z_u}}{N} \frac{1}{1 + \frac{K}{2^K N} \frac{M - M_0 Z_s}{2^K N} (M_0^0 - M_0 + Z_u - Z_s)} : \quad (32)$$

Z_u is the number of unsatisfied clauses which contains the variable to be flipped. All these clauses will become satisfied after the flip. The factor $Z_u = (K M_0)$ represents the probability of flip of the variable, the factor N coming from the sum over its index j . Z_s is the number of clauses satisfied prior to the flip and violated after. The meaning of the Binomial laws is transparent. Assume that the conformation violates M_0 clauses. In the absence of further information, the variable which is going to flip has probability K/N to be present in a given clause (there are $\binom{N}{K}$ possible K -uplets over N variables, and $\binom{N-1}{K-1}$ which include a given variable). Furthermore, a satisfied clauses that contains the flipped variable has a probability $1/2^K$ to become unsatisfied later. Z_u (respectively Z_s) is thus drawn from a binomial law with parameter K/N (resp. $K/2^K = N$), over M_0 (resp. $M - M_0$) tries. This reasoning unveils the physical significance of our Markovian approximation; we neglect all correlations between flipped variables and clauses that inevitably arise as the algorithm runs beyond the description in terms of the microscopic variable M_0 .

C. Average evolution and the metastable plateau

The evolution equation for the average fraction $\rho_0(T) = \frac{1}{M_0} \sum_{M_0} M_0 \text{Prob}[M_0; T] = M$ of unsatisfied clauses at time $T = tM$ is easily computed in the large size limit from (30,32). In particular, the average fraction of unsat clauses equals

$$\rho_0(K; t) = \frac{1}{2^K} + \frac{1}{2^K + 1} \left(\frac{2^K}{K} + \frac{1}{2^K} \right) e^{-K(1 + 2^{-K})t} - 1; \quad (33)$$

with $\rho_0(0) = 1/2^K$. Two regimes appear. If the ratio is smaller than the critical value

$$\rho_d(K) = \frac{2^K}{K}; \quad (34)$$

the average fraction of unsat clauses ρ_0 vanishes after a finite time t_{res} . Typically, the algorithm will find a solution after $t_{\text{res}} \sim M$ steps (linear in N), and then stops. Predictions for ρ_d are in good but not perfect agreement with estimates from numerical simulations e.g. $\rho_d = 8/3$ vs. $\rho_d \approx 2.7 - 2.8$ for 3-SAT. The average resolution time $t_{\text{res}}(K)$ predicted within this approximation is given by the time at $\rho_0(t)$ in eqn (33) vanishes. It logarithmically diverges as ρ_d reaches the dynamical threshold at fixed K ,

$$t_{\text{res}}(K) = \frac{1}{2^K + 1} \ln \rho_d(K); \quad \rho_d(K) > \rho_d(K); \quad (35)$$

On the contrary, when $\rho_d > \rho_d(K)$, ρ_0 converges to a finite and positive value

$$\rho_0(K) = \frac{1}{2^K + 1} - 1 - \frac{2^K}{K} \quad (36)$$

when $t \rightarrow \infty$ (Figure 3). Random WalkSAT is not able to find a solution and gets trapped at a positive level of unsatisfied clauses. This situation arises in the limit $T/N \rightarrow \infty$, and corresponds to the metastable plateau identified in Section IIC.

D . Large deviations and escape from the metastable plateau

As explained above, when $\gamma > \gamma_d$, the system gets almost surely trapped in a metastable portion of the configuration space with a non zero number of unsatisfied clauses. Numerical experiments indicate the existence of an exponentially small-in- N probability $\exp(-N \phi(\gamma))$ with $\phi(\gamma) > 0$ that this scenario is not correct, and that a solution is indeed found in a linear time. We now make use of our Markovian hypothesis to derive an approximate expression for $\phi(\gamma)$.

Contrary to the previous section, we now consider the large deviation of the process with respect to its typical behaviour. This can be accessed through the study of the large deviation function $\phi(\gamma; t)$ of the fraction γ_0 [38],

$$\phi(\gamma; t) = \lim_{N \rightarrow \infty} \frac{1}{N} \ln \text{Prob}[M_0 = M(\gamma_0); T = tN] \quad (37)$$

Introduction of the reduced time is a consequence of the following remark. $O(1)$ changes in the fraction γ_0 , that is, $O(N)$ changes in the number M_0 of unsatisfied clauses are most likely to occur after a number of flips of the order of N . To compute the large deviation function ϕ , we introduce the generating function of M_0 ,

$$G(y; T) = \sum_{M_0} \text{Prob}[M_0; T] \exp(y M_0); \quad (38)$$

where y is a real-valued number. In the thermodynamic limit, G is expected to scale exponentially with N with a rate

$$g(y; t) = \lim_{N \rightarrow \infty} \frac{1}{N} \ln G(y; T = tN) = \max_{\gamma_0} [\phi(\gamma_0; t) + y \gamma_0]; \quad (39)$$

equal to the Legendre transform of ϕ from insertion of definition (37) into eqn. (38). Using evolution equations (30,32), we obtain the following equation for g ,

$$\frac{1}{N} \frac{\partial g(y; t)}{\partial t} = y + \frac{K}{2^K} e^y (1 + K e^{-y} - 1) \frac{1}{2^K} (e^y - 1) \frac{\partial g(y; t)}{\partial y}; \quad (40)$$

along with the initial condition

$$g(y; 0) = \ln(1 + \frac{1}{2^K} + \frac{e^y}{2^K}) \quad (41)$$

The average evolution studied in the previous section can be found again from the location of the maximum of g , or, equivalently, from the derivative of g in $y = 0$: $\gamma_0(t) = (1/\gamma) \partial g / \partial y(0; t)$. The logarithm of the probability of resolution (divided by N) at times large compared to N , but very small compared to $\exp(O(N))$, is given by

$$\phi(\gamma; K) = \phi(\gamma_0 = 0; t \rightarrow \infty) = \max_{\gamma_0} \int_0^{\gamma_0} dy z(y; \gamma); \quad (42)$$

where $z(y; \gamma) = (\gamma - K(e^y - 1)) = (K(e^y - 1) - (\gamma - 1))$ and $y(\gamma)$ is the negative root of z .

Predictions for ϕ in the $K = 3$ case are plotted in Figure 9. They are compared to experimental measures of ϕ , that is, the logarithm (divided by N) of the average resolution times. It is expected on intuitive grounds exposed in Section IIC that ϕ coincides with ϕ_{th} (Figure 2). Despite the roughness of our Markovian approximation, theoretical predictions are in qualitative agreement with numerical experiments.

E . Taking into account clauses types

The calculation of Section IV B can be extended to other observables R . In the following, we consider the case of a vectorial observable M , with $K + 1$ components. Our starting point is the classification of clauses into 'types'. A clause is said to be of type i , with $i = 0; \dots; K$, if the variables of the configuration S satisfy i among K of its literals. If $i = 0$ the clause is unsatisfied while, as soon as $i \geq 1$, the clause is satisfied. Let us call $M_i(S)$ the number of clauses of type i , and $M(S) = (M_0(S); \dots; M_K(S))$ the vector made with these population sizes. Clearly, $\sum_i M_i(S) = M$ for any configuration. If $M_0(S) = 0$ then S is a solution of the formula. Vector M is a natural characterization of

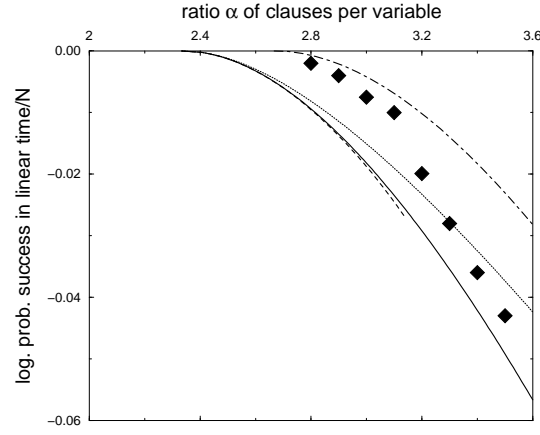


FIG. 9: Large deviations for the 3-SAT problem. The logarithm of the probability of successful resolution (over the linear in N time scale) is plotted as a function of the ratio of clauses per variables. Predictions for $(\alpha; 3)$ have been obtained within the approximations of Section IV D (equation (42), dot-dashed curve) and Section IV E (second {dotted line}, third {dashed}, quartic {solid} order solution of eqn (49)). Diamonds corresponds to (minus) the logarithm of the average resolution times (averaged over 2,000 to 10,000 samples depending on the values of $\alpha; N$, divided by N and extrapolated to $N \rightarrow 1$) obtained from numerical simulations. Error bars are smaller than the size of the diamond symbol. Schoning's bound is $\ln(3/4) \approx -0.288$.

the configuration of variables (and of the instance), and contains essential information about the operation of the algorithm. Indeed, the algorithm stops if the number M_0 of unsatisfied clauses vanishes. In addition, at each step of the algorithm, a single variable is flipped; clauses of type i become of type $i-1$ if they include this variable, remain of type i otherwise.

Within our Markovian annealed approximation, the probability $P(\tilde{M}^0; T)$ that the configuration of the variables is in class (\tilde{M}^0) at time T obeys the evolution equation,

$$P(\tilde{M}^0; T+1) = \sum_{\tilde{M}^0} \mathbb{A}_{\tilde{M}^0 \tilde{M}^0} P(\tilde{M}^0; T); \quad (43)$$

with

$$\mathbb{A}_{\tilde{M}^0 \tilde{M}^0} = \sum_Z \frac{N Z_0}{K M_0} \tilde{M}^0 \tilde{M}^0(Z) P(Z | \tilde{M}^0) \quad (44)$$

where $Z = (Z_0; Z_1; Z_1^s; \dots; Z_i; Z_i^s; \dots; Z_{K-1}; Z_{K-1}^s; Z_K)$ is a $2K+1$ dimensional vector. Component Z_i is the number of clauses of type i where the variable which is going to flip appears. In Z_i^s of these Z_i clauses, this variable was one of the i satisfying literals. It is not necessary to introduce components Z_0^s and Z_K^s for they have obvious values (respectively equal to 0 and Z_K). \mathbb{Z} denotes a $(K+1) \times (2K+1)$ matrix such that \mathbb{Z} gives the change in the observable \tilde{M} when the variable is flipped. The i th line of \mathbb{Z} reads $Z_i + Z_{i+1}^s + (Z_{i-1} - Z_{i-1}^s)$. Clauses that contain the flipped variable and were of type i prior to the flip are not any longer of this type after the flip (hence the term $-Z_i$), those which were of type $i+1$ and satisfied by the variable become of type $i + Z_{i+1}^s$, as those which were of type $i-1$ and unsatisfied by the flipping variable $(+Z_{i-1} - Z_{i-1}^s)$. The probability of Z conditioned to \tilde{M}^0 is, as in the simpler case of Section IV B a product of Binomial laws,

$$P(Z | \tilde{M}^0) = \prod_{i=0}^K \frac{M_i}{Z_i} \left(\frac{K}{N} \right)^{Z_i} \left(1 - \frac{K}{N} \right)^{M_i - Z_i} \prod_{i=1}^K \frac{Z_i}{Z_i^s} \left(\frac{1}{K} \right)^{Z_i^s} \left(1 - \frac{1}{K} \right)^{Z_i - Z_i^s}; \quad (45)$$

Repeating the procedures of Sections IV C and IV D, we find

The average fraction of unsat clauses is calculated in Appendix A and reads

$$f_0(\alpha; K; t) = \frac{1}{2^K} + \frac{1}{K} \frac{1}{(1 + \tanh(\alpha t))^K} - 1; \quad (46)$$

The critical ratio separating polynomial from exponential resolutions is

$$\alpha_d(K) = \frac{2^K - 1}{K} : \quad (47)$$

When $\alpha < \alpha_d$, the resolution time t_{res} is given by the vanishing of ρ_0 in eqn (46). Both $\alpha_d(K)$ and $t_{res}(\alpha; K)$ differ from their values found within the simpler approximation of Section IV B.

When $\alpha > \alpha_d(K)$, the average fraction of unsatisfied clauses on the plateau is given by

$$\rho_0(\alpha; K) = \frac{1}{2^K} - \frac{1}{K} \frac{2^K - 1}{K} : \quad (48)$$

Results are plotted in Figure 3.

The probability of easy (linear time) resolution is accessible from the large deviation function $\phi(\mathbf{y}; t)$ of the fractions ρ_i of clauses of type 0 $\leq i \leq K$. Its Legendre transform $g(\mathbf{y}; t)$ obeys the PDE

$$-\frac{1}{\partial t} \frac{\partial g(\mathbf{y}; t)}{\partial t} = \sum_{i=0}^K (K-i) e^{y_{i+1} - y_i} + i e^{y_{i-1} - y_i} - K \frac{\partial g(\mathbf{y}; t)}{\partial y_i} \quad (49)$$

along with the initial condition

$$g(\mathbf{y}; 0) = \ln \sum_{i=0}^K \frac{1}{2^K} \binom{K}{i} e^{y_i} : \quad (50)$$

The logarithm of the probability of resolution (divided by N) at times large compared to N , but very small compared to $\exp(N)$, is given by

$$\phi(\alpha; K) = \max_{y_0} g(y_0; y_1 = y_2 = \dots = y_K = 0; t) : \quad (51)$$

We have not been able to calculate exactly for generic values of α and K , but have resorted to a polynomial expansion of g in powers of its arguments y_i . The expansion has been done up to order 4 with the help of a symbolic computation software for $K = 3$, and up to order 2 analytically for any K . Calculations are exposed in Appendix B. Predictions for $\phi(\alpha)$ in the $K = 3$ case are plotted in Figure 9.

F. The large K limit

Comparison between results of Sections IV B and IV E shows that the output of the calculation quantitatively depends on the observable under study. However, we may expect some simplification to take place for large K . In this limit, if a clause gets unsatisfied twice, or more (but $\ll K$ times), it is very unlikely that each variable will be flipped more than once, and memory effects are lost. Therefore, the Markovian annealed approximation is expected to become correct. However, to avoid a trivial limit, the ratio of clauses per variable must be rescaled accordingly. Inspection of the above results (34,47) indicate that the correct scaling is $\alpha; K \rightarrow 1$ at fixed ratio $\alpha = K/2^K$. The dynamical threshold separating linear from exponential resolutions is located in

$$\alpha_d = 1 : \quad (52)$$

As the critical threshold of K -SAT is known to scale as $\alpha_c(K) \sim 2^K \ln 2$ for large K [33, 37], instances are always satisfiable on the reduced scale.

For $\alpha < 1$, the initial fraction of unsatisfied clauses is $\rho_0 = 1/2^K$, and decreases by $O(1)$ per unit of reduced time t , giving $t_{res} = 1/2^K$. For the same reason, the height ρ_0 , which is reached after a $O(1)$ relaxation time when $\alpha > 1$, is of the order of $1/2^K$. It is therefore natural to define the rescaled fraction of unsatisfied clauses through

$$\rho_0(\alpha; t) = \lim_{K \rightarrow \infty} 2^K \rho_0(\alpha/K; K; t/2^K) : \quad (53)$$

from which we obtain the rescaled resolution time $t_{\text{res}}(\beta)$ for $\beta < 1$ (vanishing of $\rho_0(\beta)$) and plateau height $\rho_0(\beta)$ for $\beta > 1$ (limit value of ρ_0 at large rescaled times). The two schemes of approximation of Section IV B and IV E both yield

$$\rho_0(\beta; t) = 1 + \frac{1}{2} e^{-t} - 1 \quad (54)$$

$$t_{\text{res}}(\beta) = -\frac{1}{\rho_0(\beta)} \ln \rho_0(\beta) = 1 + \frac{1}{2} \beta + \frac{1}{3} (\beta - 1)^2 + O((\beta - 1)^3) \quad (55)$$

$$\rho_0(\beta) = 1 - \frac{1}{2} = \frac{1}{2} + O((\beta - 1)^2); \quad (56)$$

Note that the small β expansion (55) for the resolution time coincides with the exact expansion obtained from eqn (22) with the above rescaling of β and K . We conjecture that the equality holds for higher orders ($\beta - 1$) in β , and that the above expressions for $\rho_0(\beta; t)$ and thus for $t_{\text{res}}(\beta); \rho_0(\beta)$ are correct.

The logarithm of the probability of linear time resolution for $\beta > \beta_d(K)$ needs to be rescaled too,

$$(\beta) = \lim_{K \rightarrow \infty} K^{-1} (\beta^{2^K} - K) \quad (57)$$

to acquire a well defined limit when $K \rightarrow \infty$. The scalar approximation of Section IV D gives the asymptotic result,

$$(\beta) = \int_0^{\gamma(\beta)} dy \frac{y (e^y - 1)}{e^y - 1} = \frac{1}{2} (\beta - 1)^2 + O((\beta - 1)^3); \quad (58)$$

where $\gamma(\beta)$ is the negative root of the numerator in the above integral. The quadratic resolution of the PDE arising from the study of Section IV E (cf. Appendix B) also leads to this result around $\beta = 1$. Unfortunately, the exact results obtained in Section III are of no help to confirm identity (58).

G. The XORSAT case

XORSAT is a version of a satisfiability problem, much simpler than SAT from a computational complexity point of view [24, 26, 35, 36]. One still draws K -uplets of variables, but each clause bears only one 'sign' (instead of one for each variable in the KSAT version), and the clause is said to be satisfied if the exclusive OR (XOR) of its boolean variables is equal to the 'sign' of the clause. For a given clause, there are 2^{K-1} satisfiable assignments of the variables, and also 2^{K-1} unsatisfiable assignments, in deep contrast with SAT where these numbers are respectively equal to $2^K - 1$ and 1. XORSAT may be recast as linear algebra problem, where a set of M equations involving N Boolean variables must be satisfied modulo 2, and is therefore solvable in polynomial time by various methods e.g. Gaussian elimination. Nevertheless, it is legitimate to ask what the performances of local search methods as Random WalkSAT are for this kind of computational problem.

A fundamental feature of XORSAT is that, whenever a spin is flipped, all clauses where this spin appears change status: the satisfied ones become unsatisfied, and vice versa. There is thus no need to distinguish between clauses satisfied by a different number of literals, and the macroscopic observable we track is the number M_0 of unsatisfied clauses for configuration S as in Section IV B. It is an easy check that the transition matrix $[A]$ for XORSAT is given by eqn (32) where 2^K is replaced with 1. Main results are:

The average fraction of unsatisfied clauses $\rho_0(t)$ reads

$$\rho_0(\beta; K; t) = \frac{1}{2} + \frac{1}{2^K} (e^{-2^K t} - 1); \quad (59)$$

and becomes asymptotically strictly positive if the ratio of clauses per variables exceeds $\beta_d(K) = 1/K$, smaller than the clustering and critical ratios, $\beta_s \approx 0.818$ and $\beta_c \approx 0.918$ for $K = 3$ respectively [24, 26]. The overall picture of the algorithm behavior is identical to the SAT case.

When $\beta > \beta_d(K)$, the average fraction of unsatisfied clauses on the plateau is given by

$$\rho_0(\beta; K) = \frac{1}{2} \left(1 - \frac{1}{K} \right); \quad (60)$$

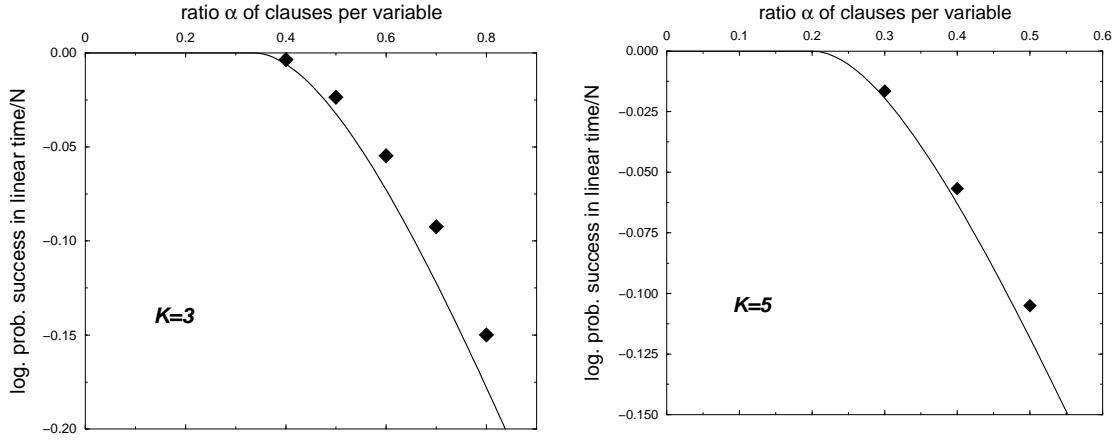


FIG. 10: Large deviations for the K-XORSAT problem for $K = 3$ (left) and $K = 5$ (right). The logarithm of the probability of successful resolution (over the linear time scale) is plotted as a function of the ratio of clauses per variables. Diamonds corresponds to $(\ln \text{ minus})$ the logarithm of the average resolution times (averaged over 10,000 samples, divided by N and extrapolated to $N \rightarrow \infty$) obtained from numerical simulations. Error bars are smaller than the size of the diamond symbol.

The partial differential equation for the generating function is,

$$\frac{1}{\partial t} g(y; t) = -y + K(e^y - 1) + K(e^y - e^y) \frac{\partial}{\partial y} g(y; t) \quad (61)$$

with $g(y; 0) = \ln[1 + e^y] = 2$. Resolution in the large time limit is straightforward, with the results shown in Figure 10. The agreement with numerics is good, especially as K grows.

The relatively simple structure of XORSAT makes possible the test of some of the approximations done. We show in Appendix C that the annealed hypothesis done in the calculation of the evolution matrix A is justified in the thermodynamic limit. The validity of this approximation in the case of 3-SAT (Section IV B) is not established for finite K .

As for K -SAT, quantities of interest have a well defined large K limit provided the ratio $\alpha = \alpha_d(K) = K$ is kept fixed;

$$\rho_0(\alpha; t) = \lim_{K \rightarrow \infty} \rho_0(\alpha = K; K; t) = \frac{1}{2} + \frac{1}{2} (e^{2\alpha t} - 1) \quad (62)$$

$$\begin{aligned} \langle \alpha \rangle &= \lim_{K \rightarrow \infty} K \langle \alpha = K; K \rangle = \int_0^\infty dy z(y; \alpha) \\ &= \frac{1}{2} (\alpha^2 + O(\alpha^3)); \end{aligned} \quad (63)$$

where $z(y; \alpha) = (y - (e^y - 1)) = (e^y - e^y)$ and $y(\alpha)$ is the negative root of z .

V. CONCLUSION AND PERSPECTIVES

In this paper, we have studied the dynamics of resolution of a simple procedure for the satisfaction of Boolean constraints, the Random WalkSAT algorithm. We have shown using complementary techniques (expansions and approximations) that, for randomly drawn input instances, Random WalkSAT may have two qualitatively distinct behaviours. Instances with small ratios of clauses per variable are almost surely solved in a time growing linearly with their size. On the contrary, for ratios above a threshold α_d , the dynamics gets trapped for an exponentially large time in a region of the configuration space with a positive fraction of unsatisfied clauses. A solution is finally reached through a large fluctuation from this metastable state.

The freezing taking place at α_d does not seem to be related to the onset of clustering between solutions[21]. Indeed the value of α_d is expected to change with the local search rules. It would be interesting to pursue the study

initiated in the present work to understand if and how the existence of this dynamical threshold is related to some property of the (static) energy landscape, as in mean field models of spin glasses [15]. Another useful improvement would be to go beyond the Markovian approximation of Section IV. Unfortunately, keeping a finite (with respect to N) number of retarded terms in (27) should not be sufficient to achieve this goal. Improvements will require to take into account an extensive number of terms, or to extend the quantum formalism of Section III to the study of the metastable phase. Another possible direction of research would be to use projection operators on observables of extensive dimension [16, 39]. Our Markovian approximation, expected to be exact in the large K limit, should be a starting point for a systematic large K expansion of the quantities of interest (plateau height, life time of the metastable regime, ...). Finally, extension of our analysis to more sophisticated local search heuristics would be useful.

Acknowledgments

We thank W. Barthel, A. K. Hartmann, M. Weigt for oral communication of their results prior to publication [16], and S. Cocco, L. Cugliandolo and A. Montanari for useful discussion and comments. The quantum formalism presented in Section III is inspired from a previous unpublished work of one of us with G. Biroli, whom we are very grateful to. We also thank C. Deroulers for his help in the perturbative resolution of eqn (49) (Section III C). The present work was partly supported by the French Ministry of Research through the ACI Jeunes Chercheurs "Algorithmes d'optimisation et systèmes désordonnés quantiques".

APPENDIX A: GENERATING FUNCTION FOR THE AVERAGE EVOLUTION

Defining $\mathcal{L} = (\ell_0; \dots; \ell_K) = \sum_{\mathbf{M}} \text{Prob}[\mathbf{M}; T] \mathbf{M} = \mathbf{M}$ and the reduced time $t = T/M$, one get from eqn (30),

$$\frac{d\mathcal{L}}{dt} = \mathbf{v} + K W_r \mathcal{L}; \quad (\text{A } 1)$$

with \mathbf{v} a $K+1$ -dimensional vector and W_r a $(K+1) \times (K+1)$ matrix defined as

$$\mathbf{v} = \begin{pmatrix} 0 \\ 1 \\ 1 \\ 0 \\ \vdots \\ 0 \end{pmatrix}; \quad W_r = \begin{pmatrix} 0 & 1 & 0 & 0 & 0 & \dots & 0 \\ 1 & \frac{1}{K} & 0 & 0 & 0 & \dots & 0 \\ 1 & 1 & \frac{2}{K} & 0 & 0 & \dots & 0 \\ 0 & \frac{K-1}{K} & 1 & \frac{3}{K} & 0 & \dots & 0 \\ \vdots & \vdots & \vdots & \vdots & \vdots & \dots & \vdots \\ 0 & 0 & 0 & 0 & \dots & \dots & 1 \end{pmatrix} \quad (\text{A } 2)$$

To solve equation (A 1), it results convenient to introduce $\langle \mathbf{x}; t \rangle$, the polynomial in \mathbf{x} whose coefficients are the fractions ℓ_i we want to determine,

$$\langle \mathbf{x}; t \rangle = \sum_{j=0}^K \ell_j(t) x^j \quad (\text{A } 3)$$

The set of $K+1$ linear coupled differential (A 1) reduces to a partial differential equation on $\langle \mathbf{x}; t \rangle$:

$$\frac{\partial}{\partial t} \langle \mathbf{x}; t \rangle = 1 + x + K(x-1)\langle \mathbf{x}; t \rangle + (1-x^2) \frac{\partial}{\partial x} \langle \mathbf{x}; t \rangle \quad (\text{A } 4)$$

At initial time, the variables are chosen randomly to be true or false, without any correlation with the formula studied. Thus, the number of satisfied literals in a clause obeys a binomial law with parameter $1/2$: $\ell_j(0) = \frac{1}{2^K} \binom{K}{j}$. The initial condition on reads thus

$$\langle \mathbf{x}; 0 \rangle = \frac{1+x}{2}^K \quad (\text{A } 5)$$

Setting $\langle \mathbf{x}; t \rangle = \langle \mathbf{x}; t \rangle + 1 = \mathcal{L}$, the constant terms in eqn (A 4) can be eliminated, with the resulting PDE for \mathcal{L} ,

$$\frac{\partial}{\partial t} \mathcal{L} = K(x-1)\mathcal{L} + (1-x^2) \frac{\partial}{\partial x} \mathcal{L} \quad (\text{A } 6)$$

This can be transformed into a wave equation on $(x;t) = (1+x)^{-K} \phi(x;t)$:

$$\frac{\partial}{\partial t} \phi(x;t) = (1-x^2) \frac{\partial}{\partial x} \phi(x;t) \quad (\text{A } 7)$$

This equation is solved in terms of an arbitrary function of a single argument,

$$\phi(x;t) = \frac{1}{2} \tanh^{-1}(x) + t \quad (\text{A } 8)$$

Knowledge of $\phi(x;0)$ for all x (A 5) allows us to determine unambiguously ϕ ,

$$\phi(u) = \frac{1}{2^K} + \frac{1}{K} [1 + \tanh(u)]^K \quad (\text{A } 9)$$

Going backwards, we obtain the expression of the generating function

$$\phi(x;t) = \frac{1+x}{2}^K + \frac{1}{K} \left(\frac{1+x \tanh(t)}{1+\tanh(t)} \right)^K \quad (\text{A } 10)$$

and of the fractions of clauses of type i through an expansion of the latter in powers of x ,

$$\phi_i(t) = \frac{1}{2^K} + \frac{1}{K} \frac{(\tanh(t))^i}{(1+\tanh(t))^K} \quad (\text{A } 11)$$

APPENDIX B: PERTURBATIVE RESOLUTION OF THE LARGE DEVIATION PDE

In this appendix we sketch the resolution of PDE (49) in the long time limit, where the function g becomes independent of time. We expand it in powers of its arguments:

$$g(y;t \rightarrow \infty) = \sum_{i=0}^K a_i y_i + \frac{1}{2} \sum_{i,j=0}^K a_{ij} y_i y_j + \dots \quad (\text{B } 1)$$

Plugging this expansion into eqn. (49), one obtains by identification of the monomials in y_i an infinite set of linear equations on the coefficients of g , which can be solved order by order. Constraint $\sum_i \phi_i = 1$ imposes a condition on g ,

$$g(y + c\mathbf{1}) = c + g(y) \quad (\text{B } 2)$$

where $\mathbf{1} = (1; 1; \dots; 1)$ and c is an arbitrary constant.

In the case $K = 3$, we have solved the set of equations on the coefficients of g up to order 4 in the y_i s with the help of a symbolic computation software. To calculate ϕ_i we need to know g as a function of y_0 only, with $y_i = 0 \forall i \neq 1$. We find

$$g(y_0) = \frac{3}{24} y_0 + \frac{105}{1920} y_0^2 + \frac{26460 + 10753}{193560} y_0^3 + \frac{29645 + 66244}{18923520} y_0^4 + O(y_0^5) \quad (\text{B } 3)$$

When $\phi_d(K=3) = 7/3$, this function has a non trivial extremum, in which g takes the value ϕ_d .

We now explain the resolution at quadratic order for a generic value of K . At linear order, following the calculation exposed in Appendix A,

$$a_i = \lim_{t \rightarrow \infty} \phi_i(t) = \frac{1}{2^K} \frac{K}{i} + \frac{1}{K} \frac{i_0}{K} \quad (\text{B } 4)$$

In particular $a_0 = \phi_d(K) = 2^{-K}$. Then considering the monomials of second order in the expansion of the equation, a set of $(K+1)(K+2)/2$ linear equations determine the coefficients a_{ij} . As we shall not try to solve the equation at higher orders for this generic case, we need only a_{00} . Again we introduce a generating function to turn the discrete algebraic problem into an analytic one. $f(s) = \sum_{i,j} a_{ij} s^{i+j}$ obeys the ordinary differential equation,

$$2K f(s) - (s+1)f'(s) = (s-1) \frac{1}{2} (1+K) \frac{1+s^2}{2} \quad (\text{B } 5)$$

with the condition $f(1) = 0$ stemming from (B2). This equation can be easily solved, yielding

$$a_{00} = f(0) = \frac{2^K}{2^{2K}} \frac{1}{K} \frac{(K-1)2^K + 2^K + 2K}{(2K-1)(2^{K-1})} \quad (B6)$$

At this order of the expansion, the extremum of g in the subspace $y_1 = 0$; $8i-1$ is reached in $y_0 = a_0 = a_{00}$ and leads to $(\beta; K) = \frac{2}{3} = (2a_{00})$.

APPENDIX C: VALIDITY OF THE ANNEALED HYPOTHESIS FOR THE XORSAT PROBLEM

We justify in this appendix the annealed average of the Markovian transition matrix in the XORSAT case. Our analysis is based on Chebyshev inequality [40]: a positive integer valued random variable with a variance negligible with respects to the square of its average is sharply peaked around its mean value. Call $D_U = \frac{1}{S} \sum_{S \in \mathcal{S}} (U - U(S))$ the number of configurations with U unsatisfied clauses. The first moment of D_U over the distribution of XORSAT instances is easy to compute. After averaging, the 2^N configurations of the variables contribute equally to the sum; for each of them, the number U of unsatisfied clause has a binomial distribution of parameter $1/2$ among the M clauses. In the thermodynamic limit, using Stirling's formula and denoting $\beta_0 = U/M$,

$$\langle D_U \rangle = e^{N f_1(\beta_0; \beta)}; \quad f_1(\beta_0; \beta) = \ln 2 + (\beta_0 \ln \beta_0 + (1 - \beta_0) \ln(1 - \beta_0) - \ln 2) \quad (C1)$$

up to polynomial corrections. Suppose that $\beta_0 < 1/2$. Call $\beta_0^{(1)}(\beta)$ the root of f_1 at fixed β . It is a growing function of β , vanishing for $\beta = 1$, and monotonously increasing to $1/2$ as β gets large. For $\beta_0 > \beta_0^{(1)}(\beta)$, f_1 is positive, and $\langle D_U \rangle$ exponentially large. When $\beta_0 < \beta_0^{(1)}(\beta)$, $\langle D_U \rangle$ is exponentially small.

Consider now the second moment $\langle D_U^2 \rangle$ and its leading behaviour $\langle D_U^2 \rangle \sim \exp[N f_2(\beta_0; \beta)]$. We introduce the generating function

$$\sum_U \langle D_U^2 \rangle e^{2xU} = \sum_{S_1, S_2} \frac{d}{2} \frac{x}{h} e^{x(U(S_1) + U(S_2)) + i(U(S_1) - U(S_2))} \quad (C2)$$

The average on the r.h.s. can be readily performed as the M clauses are drawn independently. The trace on the two configurations reduces to a sum on the Hamming distance between them. Evaluation of this sum and the integral over β by the Laplace method yields

$$\lim_{N \rightarrow \infty} \frac{1}{N} \ln \langle D_U^2 \rangle = \sup_{\beta_0} [f_2(\beta_0; \beta) - 2x\beta_0] = S(x; \beta) \quad (C3)$$

where $S(x; \beta)$ is the maximum over β_0 of

$$S(x; \beta) = \ln 2 - \ln \left[(1 - \beta_0) \ln(1 - \beta_0) + \beta_0 \ln \beta_0 + p(\cosh x - 1) \right] \quad (C4)$$

and $p_e(\beta) = (1 + (1 - 2\beta)^2)/2$ is the probability that a randomly drawn clause satisfies (or violates) two configurations at Hamming distance $d = N\beta$. We are thus left with the problem of determining $S(x; \beta)$ and of computing its Legendre transform with respects to x to obtain f_2 . As the derivative of p_e in $\beta = 1/2$ vanishes, this point is always an extremum of S . Two cases must be distinguished, depending on the value of β_0 , which sees $x \in [26, 36, 41]$:

If $\beta = 1/2$ is the global maximum of S , then $f'(\beta_0; \beta) = 2f_1(\beta_0; \beta)$, in other words $\langle D_U^2 \rangle = \langle D_U \rangle^2$. In that case it is possible to compute the polynomial corrections by expanding around the saddle point,

$$\frac{\langle D_U^2 \rangle}{\langle D_U \rangle^2} = 1 + \frac{1}{N^{K-2}} \frac{2^K}{2} (1 - 4\beta_0(1 - \beta_0)) \quad (C5)$$

If the global maximum of S is not in $\beta = 1/2$, $f > f_1$, thus $\langle D_U^2 \rangle > \langle D_U \rangle^2$.

We have computed numerically for $K = 3$ the function $\beta_0^{(2)}(\beta)$ such that for $\beta_0 > \beta_0^{(2)}(\beta)$, the global maximum of S is located in $\beta = 1/2$. It is a growing function of β , vanishing when $\beta < 0.889$ [36], and growing monotonously to $1/2$ when β diverges. The results are shown in Fig. 11 (all three curves reaches $\beta_0 = 1/2$ when $\beta \rightarrow 1$ without crossing each other). In the course of the algorithm operation, β_0 decreases from its initial value ($1/2$) down to its plateau value, and remains confined to the region in the phase diagram where the second moment method applies: $\beta_0 > \beta_0^{(2)} > \beta_0^{(1)}$. This proves that, within the Markovian approximation, the annealed average is correct: as the denominator of the transition matrix is peaked around its mean value, the numerator and denominator can be averaged separately. This analysis cannot be done in the case of K -SAT, for which the second moment fails as soon as $\beta > 0$ [41].

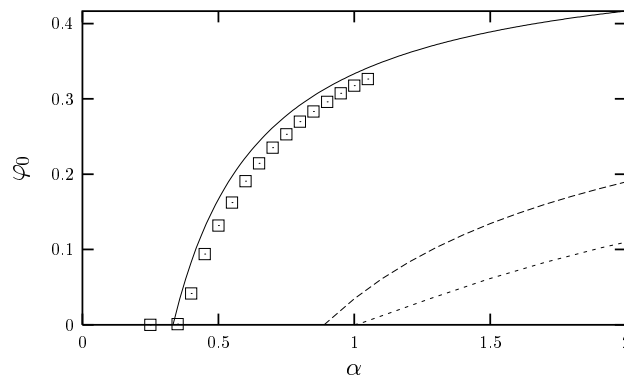


FIG. 11: Study of the moments of D_U for 3-XORSAT. Solid line: Markovian annealed prediction for the asymptotic fraction of unsat clauses ϕ_0 . Long-dashed line: $\phi_0^{(2)}$. Short-dashed line: $\phi_0^{(1)}$. Symbols: asymptotic fraction of unsat clauses on the plateau, obtained through numerical simulations.

-
- [1] C.H. Papadimitriou, K. Steiglitz, Combinatorial Optimization: Algorithms and Complexity, Prentice-Hall, Englewood Cliffs, NJ (1982).
 - [2] for a recent review, see: O. Martin, R. Monasson, R. Zecchina, Theor. Comp. Sci. 265, 3{67 (2001).
 - [3] M. Talagrand, Theor. Comp. Sci. 265, 69{77 (2001).
 - [4] D.E. Knuth, Selected Papers on Analysis of Algorithms, Stanford, California: Center for the Study of Language and Information no.102 (2000).
 - [5] R. Sedgewick, P. Flajolet, Introduction to the Analysis of Algorithms, Addison-Wesley, Boston (2001).
 - [6] D. Achlioptas, Theor. Comp. Sci. 265, 159{185 (2001).
 - [7] S. Cocco, R. Monasson, Phys. Rev. Lett. 86, 1654 (2001); Eur. Phys. J. B 22, 505 (2001).
 - [8] S. Cocco, R. Monasson, Phys. Rev. E 66, 037101 (2002).
 - [9] M. Weigt, A. Hartmann, Phys. Rev. Lett. 86, 1658 (2001).
 - [10] A. Montanari, R. Zecchina, Phys. Rev. Lett. 88, 178701 (2002).
 - [11] R. Motwani, P. Raghavan, Randomized Algorithms, Cambridge University Press, Cambridge (1995).
 - [12] C.H. Papadimitriou, Proceedings of the 32nd Annual IEEE Symposium on Foundations of Computer Science, 163 (1991).
 - [13] D. Mitchell, B. Selman, H. Levesque, Proc. of the Tenth Natl. Conf. on Artificial Intelligence (AAAI-92), 440-446 (The AAAI Press / MIT Press, Cambridge, MA, 1992).
 - [14] T.M. Liggett, Stochastic Interacting Systems: Contact, Voter and Exclusion Processes, Springer-Verlag, Berlin (1999).
 - [15] L.F. Cugliandolo, Dynamics of glassy systems", Lecture notes, Les Houches, preprint cond-mat/0210312 (2002).
 - [16] W. Barthel, A. Hartmann, M. Weigt, "Solving satisfiability problems by fluctuations: An approximate description of the dynamics of stochastic local search algorithms", preprint (2003).
 - [17] E. Friedgut, J. Amer. Math. Soc. 12, 1017{1054 (1999).
 - [18] A.C. Kaporis, L.M. Kourousis, E.G. Lalas, "The Probabilistic Analysis of a Greedy Satisfiability Algorithm", European Symposium on Algorithms, 574{585 (2002).
 - [19] O. Dubois, Y. Boufkhad, J. Mandler, "Typical random 3-SAT formulae and the satisfiability threshold", SODA 2002, 126-127 (2002).
 - [20] for a review on random 2-SAT, see: F. De la Vega, Theor. Comp. Sci. 265, 131{146 (2001).
 - [21] G. Biroli, R. Monasson, M. Weigt, Eur. Phys. J. B 14, 551 (2000).
 - [22] M. Mezard, G. Parisi, R. Zecchina, Science 297, 812 (2002). M. Mezard, R. Zecchina, Phys. Rev. E 66, 056126 (2002).
 - [23] for a recent review, see: A. Engel, C. Van den Broeck, Statistical mechanics of learning, Cambridge University Press, Cambridge (2000).
 - [24] F. Ricci-Tersinghi, M. Weigt, R. Zecchina, Phys. Rev. E 63, 026702 (1999). S. Franz et al., Phys. Rev. Lett. 87, 127209 (2001).
 - [25] R. Mulet, A. Pagnani, M. Weigt, R. Zecchina, Phys. Rev. Lett. 89, 268701 (2002).
 - [26] O. Dubois, J. Mandler, "The 3-XORSAT threshold", Proc. of the 43rd annual IEEE symposium on Foundations of Computer Science, Vancouver (2002). S. Cocco, O. Dubois, J. Mandler, R. Monasson, "Rigorous decimation-based construction of ground pure states for spin glass models on random lattices.", preprint cond-mat/0206239, to appear in Phys. Rev. Lett. (2002).

- M. Mezard, F. Ricci-Tersenghi, R. Zecchina, "Alternative solutions to diluted p-spin models and XOR SAT problems", preprint cond-mat/0207140 (2002).
- [27] C.M. Newman, D.L. Stein, Phys. Rev. E 55, 5194-5211 (1998), and in "Mathematical Aspects of Spin Glasses and Neural Networks", A. Bovier, P. Picco, eds., Birkhauser, Boston, 243-287 (1998).
- [28] P. Svensson, M.G. Nordahl, Phys. Rev. E 59, 3983 (1999).
- [29] U. Schoning, Algorithmica 32, 615-623 (2002).
- [30] M. Alekhnovich, E. Ben-Sasson, "Analysis of the Random Walk Algorithm on Random 3-CNFs", preprint (2002).
- [31] A.J. Parkes, Lecture Notes in Computer Science 2470, 708 (2002).
- [32] L.P. Kadanoff, J. Swift, Phys. Rev. 165, 310 (1968).
- [33] R. Monasson, R. Zecchina, Phys. Rev. E 56, 1357 (1997).
- [34] G. Semerjian, L.F. Cugliandolo, Phys. Rev. E 64, 036115 (2001).
- [35] N. Creignou, H. Daude, Discrete Applied Mathematics 96-97, 41 (1999).
- [36] N. Creignou, H. Daude, O. Dubois, "Approximating the satisfiability threshold for random k-XOR-formulas", preprint arXiv:cs.DM/0106001 (2001).
- [37] D. Achlioptas, Y. Peres, The Threshold for Random k-SAT is $2^k (\ln 2 + o(1))$, preprint (2002).
- [38] R.B. Griffiths, C-Y. Wang, J.S. Langer, Phys. Rev. 149, 301 (1966).
- [39] S.N. Laughton, A.C.C. Coolen, D. Sherrington, J. Phys. A 29, 763 (1996).
- [40] N. Alon, J. Spencer, The probabilistic method, John Wiley, New York (2000).
- [41] D. Achlioptas, C. Moore, The Asymptotic Order of the Random k-SAT Threshold, In Proceedings of 43rd Annual Symposium on Foundations of Computer Science (FOCS'02), Vancouver, BC, Canada, p.779-788 (2002).